

Control of the Photophysical Properties of Polyatomic Molecules by Substitution and Solvation: The Second Excited Singlet State of Azulene

Nicolas Tétreault,[†] Rajeev S. Muthyala,[‡] Robert S. H. Liu,[‡] and Ronald P. Steer*[†]

Department of Chemistry, University of Saskatchewan, 110 Science Place, Saskatoon, SK, Canada S7N 5C9, and Department of Chemistry, University of Hawaii, Honolulu, Hawaii 96822

Received: November 11, 1998; In Final Form: February 2, 1999

The UV–visible–near-IR absorption spectra, $S_2 \rightarrow S_0$ fluorescence quantum yields and S_2 fluorescence lifetimes of 1-fluoroazulene, 1,3-difluoroazulene, and several of their alkyl-substituted derivatives have been measured at room temperature in up to six solvents, benzene, dichloromethane, ethanol, acetonitrile, *n*-hexane, and perfluoro-*n*-hexane. The quantum yields (up to 0.2) and lifetimes (up to 9.5 ns) of the S_2 state of 1,3-difluoroazulene are exceptionally large—the largest ever reported for an upper excited singlet state of a polyatomic molecule with a closed-shell ground state. The nonradiative rate constants for the decay of the S_2 states of these molecules in these solvents and of azulene, 1,3-dichloroazulene and 1,3-dibromoazulene, determined previously, have been analyzed in terms of the weak coupling case of radiationless transition theory. The data show that the nonradiative rate constants for the S_2 states of azulene, 1-fluoroazulene, and 1,3-difluoroazulene in the nonpolar solvents follow the log–linear relationship expected of the energy gap law, provided that S_2 – S_1 internal conversion is assumed to dominate the decay mechanism. The same linear correlation is obtained, irrespective of whether $\Delta E(S_2$ – $S_1)$ is varied by solvatochromism or fluorine substitution. Substitution by alkyl groups increases the nonradiative decay rates by increasing the effective number of coupled states while the electronic coupling matrix element remains constant. Substitution at the 6-position by an isopropyl group increases the rate constant by a constant factor of 2.9; however, multiple substitution does not have a multiplicative effect. Substitution by chlorine or bromine increases the S_2 decay rates by enhancing the rate of intersystem crossing to the triplet manifold. The rate enhancement is semiquantitatively modeled by considering the effects of spin–orbit coupling of the halogen atoms.

Introduction

Azulene is the first-described and best-known case of a closed-shell polyatomic molecule which exhibits “anomalous” fluorescence from its second excited singlet state in condensed media at room temperature, in contravention of Kasha’s rule.^{1,2} Because azulene and its derivatives continue to serve as models for other anomalous systems, there has been a sustained interest in describing their photophysical properties quantitatively, with the aim of finding correlations which will enable the prediction of the properties of highly excited states in unknown systems. Although many attempts^{3–11} have been made to find reliable structure–property correlations, success to date has been modest.

The second excited singlet state of azulene (S_2 of 1A_1 character, when applying the C_{2v} point group to the time-averaged skeletal structure) may decay radiatively to both S_1 (1B_1 , non-Mulliken convention) and $S_0(^1A_1)$. However, the former exhibits only a minute quantum yield of fluorescence and contributes negligibly to the overall rate of S_2 s decay.¹² The remaining intramolecular decay paths of S_2 are nonradiative; internal conversion to high vibrational levels of S_1 and S_0 and intersystem crossing to the triplet manifold. There is substantial evidence¹¹ based on the energy gap law¹³ that S_2 – S_1 internal conversion is the major process by which S_2 relaxes in condensed media at room temperature in which decay from a

fully thermalized set of vibrational states is expected, irrespective of $S_2 \leftarrow S_0$ excitation wavelength. However, S_2 – S_0 internal conversion is also possible and there is some evidence that this process becomes important at high vibrational levels in S_2 .¹⁴ Evidence of S_2 – T_n intersystem crossing is also found in chlorine-, bromine-, and iodine-substituted azulene derivatives,^{4,5,11} but there is no reliable estimate of the contribution of intersystem crossing to the relaxation of the thermalized S_2 state of azulene itself.

Recently we returned to the problem of characterizing the dynamics of the S_2 state of azulene and its simple derivatives by measuring the $S_2 \rightarrow S_0$ fluorescence quantum yields and S_2 lifetimes of several series of structurally related compounds in several different solvents.¹¹ Although rather more accurate data were obtained in this study by using picosecond laser techniques and more refined quantum yield measurements,¹⁵ and the effect of solvation was established, it was still not possible to obtain meaningful energy gap law correlations using the available derivatives. Fortunately, the synthesis of new fluorinated azulenes has been reported recently.¹⁶ These new compounds provide the possibility of measuring the radiative and nonradiative decay constants of the S_2 states of several series of structurally similar compounds over a much wider range of S_2 – S_1 electronic energy spacings than has heretofore been possible, and hence of determining if the energy gap law of radiationless transition theory actually does provide a reliable basis for predicting their excited state properties. The results are reported in this paper.

* To whom correspondence should be addressed.

[†] University of Saskatchewan.

[‡] University of Hawaii.

Experimental Section

1-Fluoroazulene (FAZ), 1,3-difluoroazulene (DFAZ), 6-isopropylazulene (IAZ), 1-fluoro-6-isopropylazulene (IFAZ), 1,3-difluoro-6-isopropylazulene (IDFAZ), and fluoroguaiazulene (FGAZ, 1,4-dimethyl-3-fluoro-7-isopropylazulene) were prepared and purified as previously described.¹⁶ Benzene (B, BDH Omnisolv), acetonitrile (MeCN, Aldrich), dichloromethane (DCM, BDH Omnisolv), *n*-hexane (H, Fisher Chemicals), and ethanol (EtOH, 99.8%, Aldrich) were used as received. Perfluoro-*n*-hexane (PFH, 99%, PCR Chemicals) was fractionally distilled before use to remove fluorescent impurities.

Absorption spectra were measured on a Cary 1 spectrophotometer, using pure solvent in a matched cell as a reference. Molar absorptivities at the excitation wavelength were obtained by making precise absorbance measurements as a function of concentration and taking the slopes of the resulting linear regressions of the data from the origin. The excited-state electronic energies of each compound in the solvent in question were determined from the wavelengths of the maxima of clearly resolved 0–0 bands in the $S_1 \leftarrow S_0$ and $S_2 \leftarrow S_0$ absorption spectra.

A previously described relative method¹⁷ was used to determine the fluorescence quantum yields. Quinine bisulfate in 0.5 M aqueous H_2SO_4 ($\phi_f = 0.546^{16}$) was used as the standard and the required “ n^2 ” refractive index corrections for sample and standard solutions were employed.¹⁶ A 1 cm square quartz cuvette was used for these measurements, and the concentrations of the sample and reference were chosen so that the solutions exhibited nearly equal absorbances of ca. 0.1 or less at the excitation wavelength in order to avoid self-absorption errors and geometric artifacts. All quantum yield measurements were performed in air-saturated solutions at room temperature. Removing oxygen had a small effect on the lifetimes of some samples, and in these cases the quantum yields were corrected accordingly by multiplying the measured value by the ratio of the lifetime in deoxygenated solution to that in air-saturated solution, all other factors being the same. The maximum error in the quantum yield measurements is estimated to be $\pm 5\%$.

A Spectra-Physics synchronously pumped, cavity-dumped, frequency-doubled DCM dye laser excitation system which has been described in detail previously^{18,19} was used for the fluorescence decay time measurements. In the present experiments a cooled Hamamatsu R2809U-07 microchannel plate photomultiplier tube coupled to a Hamamatsu C4267 fast preamplifier and a modified Tennelec TC 454 constant fraction discriminator were employed in the time-correlated, single-photon detection system. An excitation wavelength of 328 nm was used throughout and emission was viewed through a Zeiss M4QIII quartz prism monochromator set at the wavelength of maximum emission intensity of each compound (ca. 380 nm). This system has an instrument response function with a fwhm of ca. 90 ps and can be used to resolve fluorescence lifetimes as short as ca. 20 ps with moderate accuracy. The maximum error in the nanosecond lifetimes recovered in these experiments is estimated to be ± 30 ps.

Solutions of 10^{-4} – 10^{-5} M concentration were employed for both the quantum yield and lifetime measurements, and data were taken only on those solutions which were sufficiently dilute that no concentration quenching could be observed on the lifetimes. The effect on the lifetimes of deoxygenating the solutions was investigated; all the lifetimes reported were measured using solutions which were purged with dry N_2 immediately prior to use. All experiments were performed at 23 ± 1 °C.

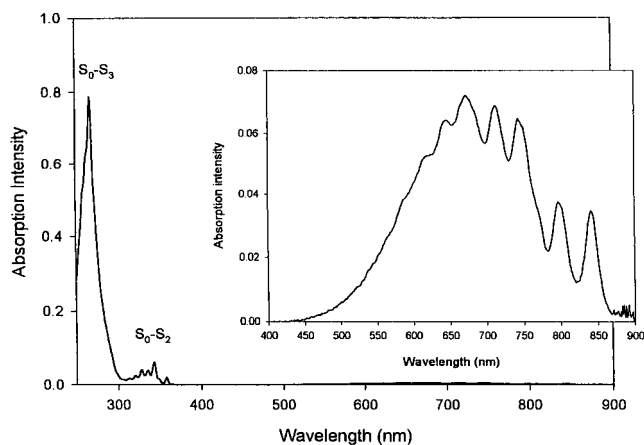


Figure 1. Representative UV–visible–near-IR absorption spectrum of 1,3-difluoroazulene in *n*-hexane at room temperature. The inset shows the S_1 – S_0 band system in more detail.

TABLE 1: Molar Absorptivity at Wavelength of Maximum Absorbance in *n*-Hexane

| compd | $\lambda_{\max}(S_2 \leftarrow S_0)$ (nm) | $\epsilon(S_2 \leftarrow S_0)$ ($M^{-1} \text{ cm}^{-1}$) | $\lambda_{\max}(S_1 \leftarrow S_0)$ (nm) | $\epsilon(S_1 \leftarrow S_0)$ ($M^{-1} \text{ cm}^{-1}$) |
|-------|--|--|--|--|
| FAZ | 343 | 3.26×10^3 | 625 | 3.23×10^2 |
| DFAZ | 342 | 3.29×10^3 | 670 | 1.44×10^2 |
| IAZ | 344 | 3.86×10^3 | 566 | 1.88×10^2 |
| IFAZ | 347 | 3.33×10^3 | 611 | 2.60×10^2 |
| IDFAZ | 347 | 2.75×10^3 | 656 | 1.92×10^2 |
| FGAZ | 348 | 4.48×10^3 | 646 | 4.31×10^2 |

Results and Discussion

The six solvents employed in this work, benzene (B), acetonitrile (MeCN), dichloromethane (DCM), *n*-hexane (H), ethanol (EtOH), and perfluoro-*n*-hexane (PFH), were chosen to provide accurately measurable solvatochromic variations in the S_2 – S_1 and S_2 – S_0 electronic energy spacings in the fluorinated azulene derivatives under study. Solvents containing atoms heavier than chlorine were excluded in order to avoid induced intersystem crossing effects.²⁰ The absorption spectrum, S_2 – S_0 fluorescence quantum yield, and S_2 lifetime of each solute were measured as a function of concentration in *n*-hexane, and these parameters were measured for FAZ and DFAZ in all six solvents. Figure 1 is a representative absorption spectrum (for 1,3-difluoroazulene in *n*-hexane), showing that the origin bands of the S_1 – S_0 and S_2 – S_0 transitions are sufficiently well resolved to provide accurate excited state energies. Table 1 lists the wavelengths and molar absorptivities at the S_1 – S_0 and S_2 – S_0 absorption maxima for the five fluorinated azulenes and 6-isopropylazulene in *n*-hexane.

Figure 2 is a representative plot of the logarithm of the relative fluorescence intensity vs time, from which the lifetimes of the S_2 states, $\tau(S_2)$, were obtained by iterative reconvolution of the measured instrument response function with trial single-exponential sample fluorescence decay functions. (Note that $\log I$ is plotted vs time, where I is normalized to the maximum number of counts per channel, typically ca. 10^4 .) The values of $E(S_2)$, $E(S_1)$, $\tau(S_2)$, and $\phi_f(S_2 \rightarrow S_0)$ are summarized in Table 2, which also reproduces the results previously obtained by Wagner et al.¹¹ for azulene (AZ), azulene- d_8 (AZ- d_8), 1,3-dichloroazulene (DCAZ), 1,3-dibromoazulene (DBAZ), and guaiazulene (GAZ). These results, all obtained with the same apparatus using the same methods, form the basis for further analysis of the radiationless decay rates of the S_2 states of these compounds. Note the large quantum yields of $S_2 \rightarrow S_0$ fluorescence (ϕ_f up to 0.20) and the long S_2 lifetimes (τ up to 9.5 ns) of DFAZ.

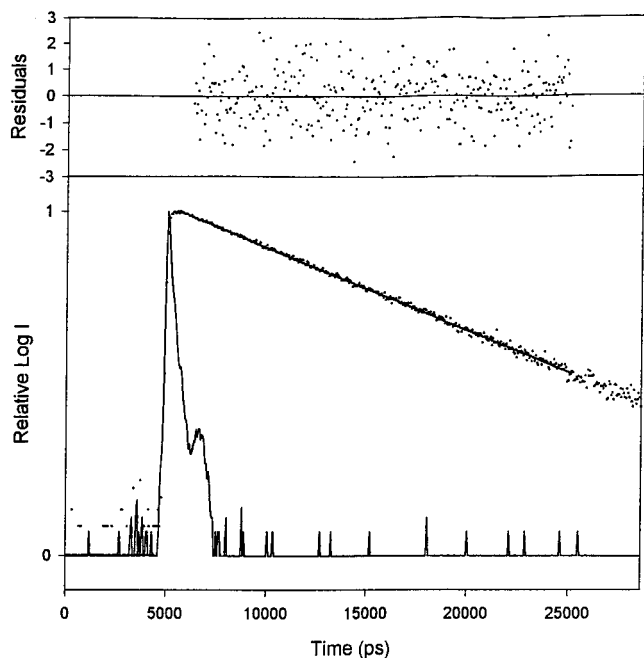


Figure 2. Representative plot of $\log I$ vs time for the decay of the S_2 state of 1,3-difluoroazulene excited at 332 nm in *n*-hexane at room temperature. The observation wavelength is centered at 378 nm, the concentration of the fluorophore is 1.87×10^{-5} M, and 10 000 counts are accumulated in the peak channel. The instrument response function is the sharply peaked solid line. The solid curve is the best fit to the measured data points of a single-exponential decay function with $\tau = 5.12$ ns convoluted with the instrument response function. The upper panel gives the distribution of weighted residuals from which a value of $\chi^2 = 0.97$ is obtained. The fit is truncated at that channel in which the background equals one-half of the signal.

We believe these are the largest values of ϕ_f and τ ever observed for an upper excited singlet state of a polyatomic organic molecule in solution at room temperature.

The rate constant for the radiative decay of S_2 , k_r , and the sum of the rate constants for all parallel first-order nonradiative decay processes of S_2 , $\sum k_{nr}$, were calculated using the standard expressions

$$k_r = \phi_f / \tau \quad (1)$$

$$\sum k_{nr} = (1 - \phi_f) / \tau \quad (2)$$

where it is understood that $\sum k_{nr}$ is the sum of all first-order and nonradiative pseudo-first-order rate processes by which S_2 decays under the conditions of the experiment. In the present work, pseudo-first-order process such as concentration quenching and quenching by oxygen have been eliminated and the compounds are all photochemically stable, so the sum here involves only the parallel intramolecular internal conversion and intersystem crossing processes of the thermally equilibrated S_2 state of each compound in each solvent. The observation of fluorescence lifetimes which could be well modeled by monoexponential fluorescence decay functions is consistent with this interpretation of the kinetics of S_2 's relaxation. The values of k_r , $\sum k_{nr}$, and $\Delta E(S_2-S_1)$ thus calculated from the primary data are also presented in Table 2.

The nanosecond S_2 fluorescence lifetimes of FAZ, DFAZ, IFAZ, IDFAZ, and FGAZ measured in the present work are reproducible to within about 30 ps, whereas that for IAZ, the shortest lived of the six solutes, is reproducible to within ca. 15 ps. The fluorescence quantum yield of each compound is

believed to be accurate to within 5%. Because the quantum yields are all < 0.2 , the precision of the values of k_r and $\sum k_{nr}$ is therefore determined primarily by the precision of ϕ_f and τ , respectively. The precision in measuring the excited state energies of the S_1 and S_2 states is typically ca. 20 and 40 cm^{-1} , respectively, so the estimated maximum error in $\Delta E(S_2-S_1)$ is ca. 60 cm^{-1} . The only exception to this is FGAZ (and GAZ itself) in which poor resolution of the S_1-S_0 and S_2-S_0 vibronic band envelopes produced by the several rotors in the molecule cause the uncertainties in $\Delta E(S_2-S_1)$ to be at least an order of magnitude larger than those of the other compounds.

Note that $\Delta E(S_2-S_1)$ is larger for FAZ compared with AZ itself, and is larger still for DFAZ. This is due almost exclusively to changes in the energies of the S_1 states because the S_2 states have energies which are only weak functions of the nature and positions of the substituents, at least for the compounds examined here. The reasons for these trends are related to the quantum mechanical descriptions of the S_1 and S_2 states in azulene and other nonalternant aromatic molecules.²¹⁻²⁴ The S_1-S_0 transition in azulene is usefully described as an electric-dipole allowed HOMO-LUMO one-electron transition which has a low oscillator strength because HOMO and LUMO have large amplitudes on different atoms and their overlap is small. Its transition dipole is perpendicular to the long axis of the azulene ring system. The S_2-S_0 transition is also electric-dipole allowed, but has a transition dipole parallel to the long axis and arises from the in-phase superposition of two one-electron transitions. Neither of these one-electron transitions has a large oscillator strength owing to their small associated charge separations, and thus the S_2-S_0 band system gains most of its intensity by vibronic coupling with higher electronic states. Both mono- and disubstitution of azulene by fluorine will withdraw electron density from the rings, and the 1- and 1,3-substitution patterns will favor stabilization of S_1 (which has an orbital symmetry which is different from S_0 and S_2) relative to either S_0 or S_2 (which have the same orbital symmetry).²³ Note that the effect on $\Delta E(S_1-S_0)$ of 1,3-disubstitution is almost exactly twice that of 1-monosubstitution; i.e., the effects of multiple fluorine substitution at equivalent sites are additive, as expected of a purely inductive effect. The fact that 1,3-disubstitution preserves C_{2v} skeletal symmetry, distorting the HOMO and LUMO electron distributions symmetrically and preserving the 1B_1 character of the S_1 state, is reflected in the considerably lower oscillator strength of the S_1-S_0 transition in 1,3-difluoroazulene compared with 1-fluoroazulene (cf. the values of ϵ in Table 1).

The radiative rate constants for S_2-S_0 fluorescence decay tend to vary qualitatively in proportion to the values of ϵ_{max} of each compound in the same solvent. However, a quantitative direct proportionality is not expected²⁵ since this transition gains most of its oscillator strength by intensity "borrowing" (in the Herzberg-Teller formalism²⁶) from the stronger nearby S_n-S_0 transitions,²² particularly that for which $n = 4$.

The radiationless decay data can be analyzed within the framework of the weak coupling, statistical limit case of the theory of radiationless transitions.^{27,28} In this model, the rate of a single process of radiationless decay of an excited electronic state is expressed most simply by the Golden Rule expression

$$k_{nr} = (2\pi/\hbar)C^2\rho F \quad (3)$$

where C is the matrix element coupling the initial and final electronic states, ρ is the density of final states, and F is the (average) Franck-Condon factor for the transition. For electronic states which are sufficiently widely spaced in a series of

TABLE 2: Experimental Results for the Nonradiative Decay of the S₂ State of Azulene and Its Derivatives in Several Solvents

| compd | solvent | $E(S_2)/10^3 \text{ cm}^{-1}$ | $E(S_1)/10^3 \text{ cm}^{-1}$ | $\Delta E(S_2-S_1)/10^3 \text{ cm}^{-1}$ | ϕ_F | τ_2/ps | $k_r/10^7 \text{ s}^{-1}$ | $\sum k_{nr}/10^8 \text{ s}^{-1}$ | $\log(\sum k_{nr})$ |
|--------------------------------|---------|-------------------------------|-------------------------------|--|----------|--------------------|---------------------------|-----------------------------------|---------------------|
| AZ ^a | PFCH | 28.65 | 14.39 | 14.26 | 0.052 | 1670 | 3.1 | 5.68 | 8.754 |
| | CH | 28.38 | 14.37 | 14.01 | 0.046 | 1330 | 3.5 | 7.17 | 8.856 |
| | EtOH | 28.51 | 14.52 | 13.99 | 0.041 | 1310 | 3.1 | 7.32 | 8.865 |
| | MeCN | 28.61 | 14.66 | 13.95 | 0.040 | 1350 | 3.0 | 7.11 | 8.852 |
| | DCM | 28.45 | 14.62 | 13.83 | 0.041 | 1170 | 3.5 | 8.20 | 8.914 |
| FAZ | B | 28.28 | 14.50 | 13.78 | 0.047 | 1040 | 4.5 | 9.16 | 8.962 |
| | PFH | 28.27 | 13.04 | 15.23 | 0.0398 | 2390 | 1.67 | 4.02 | 8.604 |
| | H | 28.01 | 13.02 | 14.97 | 0.0567 | 2430 | 2.33 | 3.88 | 8.589 |
| | EtOH | 28.14 | 13.20 | 14.94 | 0.0579 | 2460 | 2.35 | 3.83 | 8.583 |
| | MeCN | 28.23 | 13.40 | 14.83 | 0.0486 | 2280 | 2.13 | 4.17 | 8.620 |
| DFAZ | DCM | 28.06 | 13.32 | 14.74 | 0.0607 | 2630 | 2.31 | 3.57 | 8.553 |
| | B | 28.00 | 13.18 | 14.82 | 0.0606 | 2060 | 2.94 | 4.56 | 8.659 |
| | PFH | 28.21 | 11.86 | 16.35 | 0.126 | 8440 | 1.49 | 1.04 | 8.015 |
| | H | 28.01 | 11.88 | 16.13 | 0.147 | 6860 | 2.14 | 1.24 | 8.095 |
| | EtOH | 28.12 | 12.09 | 16.03 | 0.197 | 9450 | 2.08 | 0.850 | 7.929 |
| AZ-d ₈ ^a | MeCN | 28.21 | 12.30 | 15.91 | 0.136 | 7450 | 1.83 | 1.16 | 8.064 |
| | DCM | 28.03 | 12.17 | 15.86 | 0.158 | 8840 | 1.79 | 0.952 | 7.979 |
| | B | 27.97 | 12.07 | 15.90 | 0.155 | 6490 | 2.39 | 1.30 | 8.115 |
| | PFCH | 28.74 | 14.40 | 14.34 | 0.067 | 2230 | 3.0 | 4.18 | 8.621 |
| | CH | 28.45 | 14.39 | 14.05 | 0.072 | 1710 | 4.2 | 5.43 | 8.735 |
| IAZ | EtOH | 28.58 | 14.56 | 14.02 | 0.060 | 1660 | 3.6 | 5.66 | 8.753 |
| | MeCN | 28.61 | 14.62 | 13.99 | 0.058 | 1680 | 3.5 | 5.60 | 8.748 |
| | DCM | 28.49 | 14.62 | 13.87 | 0.066 | 1480 | 4.4 | 6.31 | 8.800 |
| | B | 28.38 | 14.54 | 13.84 | 0.073 | 1360 | 5.4 | 6.81 | 8.833 |
| | H | 29.07 | 14.66 | 14.41 | 0.0131 | 510 | 2.57 | 19.4 | 9.287 |
| IFAZ | H | 28.82 | 13.43 | 15.39 | 0.0191 | 940 | 2.03 | 10.4 | 9.017 |
| IDFAZ | H | 28.82 | 12.26 | 16.56 | 0.0508 | 2690 | 1.89 | 3.53 | 8.548 |
| GAZ ^a | PFCH | 27.4 | 13.8 | 13.7 | 0.013 | 260 | 5.0 | 37.9 | 9.579 |
| | CH | 27.2 | 13.7 | 13.5 | 0.018 | 330 | 5.4 | 29.8 | 9.474 |
| | EtOH | 27.4 | 13.8 | 13.6 | 0.017 | 330 | 5.1 | 29.8 | 9.474 |
| | MeCN | 27.4 | 13.9 | 13.5 | 0.017 | 350 | 4.9 | 28.1 | 9.449 |
| | DCM | 27.3 | 14.0 | 13.3 | 0.022 | 290 | 8.6 | 33.7 | 9.528 |
| FGAZ | B | 27.1 | 13.8 | 13.3 | 0.021 | 290 | 7.2 | 33.8 | 9.529 |
| | H | 27.4 | 12.6 | 14.8 | 0.0914 | 1910 | 4.79 | 4.76 | 8.677 |
| | PFCH | 27.40 | 12.77 | 14.63 | 0.082 | 1370 | 6.0 | 6.70 | 8.826 |
| | CH | 27.14 | 12.79 | 14.35 | 0.073 | 990 | 7.4 | 9.36 | 8.971 |
| | EtOH | 27.40 | 13.10 | 14.30 | 0.062 | 880 | 7.0 | 10.7 | 9.029 |
| DCAZ ^a | MeCN | 27.41 | 13.21 | 14.20 | 0.053 | 810 | 6.5 | 11.7 | 9.068 |
| | DCM | 27.24 | 13.17 | 14.07 | 0.056 | 740 | 7.6 | 12.8 | 9.107 |
| | B | 27.14 | 13.09 | 14.05 | 0.057 | 710 | 8.1 | 13.3 | 9.124 |
| | CH | 27.03 | 13.16 | 13.87 | 0.016 | 200 | 8.0 | 49.2 | 9.692 |
| | B | 27.03 | 13.35 | 13.68 | 0.013 | 180 | 7.2 | 54.8 | 9.739 |
| TMAZ ^a | PFCH | 28.00 | 15.48 | 12.52 | 0.0006 | 17 | 3.5 | 590 | 10.771 |
| | CH | 27.82 | 15.53 | 12.29 | 0.0005 | 15 | 3.3 | 670 | 10.826 |
| | EtOH | 27.78 | 15.78 | 12.00 | 0.0005 | 14 | 3.2 | 710 | 10.851 |
| | B | 27.62 | 15.65 | 11.97 | 0.0005 | 12 | 4.2 | 830 | 10.919 |
| | DCM | 27.74 | 15.90 | 11.84 | 0.0004 | ≤10 | | | |
| MeCH | 27.72 | 15.90 | 11.82 | 0.0003 | ≤10 | | | | |

^a From ref 11. H, *n*-hexane; B, benzene; CH, cyclohexane, EtOH, ethanol; PFCH, perfluorocyclohexane; PFH, perfluoro-*n*-hexane; MeCN, acetonitrile; DCM, dichloromethane.

structurally similar molecules, F varies approximately as the exponent of the inverse of the electronic energy gap, ΔE , leading to the “energy gap law” of radiationless transition theory,¹³

$$\log(k_{nr}) \propto \log(F) \propto -\Delta E \quad (4)$$

Thus, for a series of structurally similar compounds in which an excited state decays by a single radiationless decay process, $\log(k_{nr})$ should be a linear function of ΔE . A good linear relationship between experimentally determined values of $\log(k_{nr})$ and ΔE for a pair of electronic states can be taken as *prima facie* evidence that one radiationless process dominates the excited state’s decay and that the weak-coupling model is valid for the system.

One can ensure the validity of applying the energy gap law to a particular system by taking data on the same compound in several solvents, i.e., by using only solvatochromic effects to cause variations in ΔE and k_{nr} . Not all solvents may be suitable, since heavy atom-containing solvents can enhance spin-orbit

coupling in the chromophore,²⁰ and specific dipolar solute-solvent interactions can also cause changes in parameters other than the spacings of its electronic energies. Moreover, solvatochromic effects produce relatively small variations in ΔE , and it is therefore important to find a series of structurally similar molecules in which ΔE varies substantially. If such a series can be found, then the validity of an analysis of the rates of radiationless decay in terms of the energy gap law can be tested by varying ΔE for several compounds in several suitable solvents.

Azulene and its two fluorinated derivatives, FAZ and DFAZ, in several nonpolar solvents appear to fit these requirements nicely. First, all three compounds are structurally rigid, so that any effects on the radiationless decay rates due to the presence of flexible or rotating substituents are avoided. Second, the rates of radiationless processes involving the S₂ state are known to be a weak function of the number of C-H oscillators in the molecule,^{8,9} since the effect of perdeuteration of azulene is a

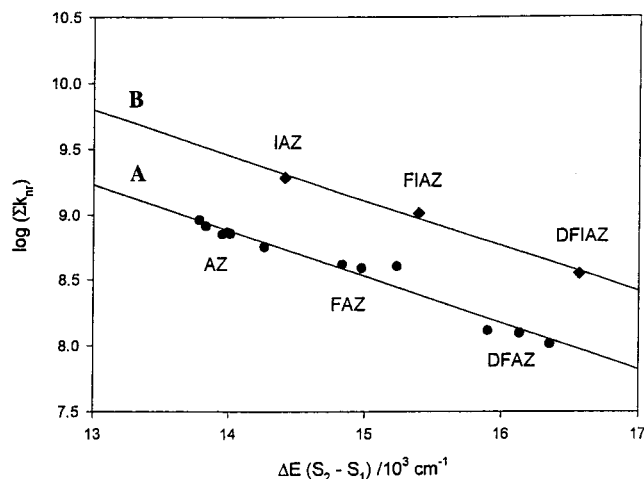


Figure 3. Log-linear energy gap law plots (see text) for azulene (AZ), 1-fluoroazulene (FAZ), and 1,3-difluoroazulene (DFAZ) in several solvents (line A), and for 6-isopropylazulene (IAZ), 1-fluoro-6-isopropylazulene (FIAZ), and 1,3-difluoro-6-isopropylazulene in *n*-hexane (line B). The data for AZ in several solvents are taken from ref 11.

reduction in the radiationless decay rate by only a factor of 1.3.¹¹ The implication is that, unlike the S_1 and T_1 states of alternant aromatic hydrocarbons,²⁹ the most important accepting/promoting modes in the radiationless decay of the S_2 state of azulene (and presumably its derivatives) are not high-frequency C–H stretches, but rather are C–C skeletal deformation modes. Fluorine mono- or disubstitution is therefore expected to have a minimal effect on the number and type of the vibrational modes involved in the radiationless decay of azulene's S_2 state. Third, fluorine is a “light” atom, and would not be expected to significantly increase the rate of intersystem crossing by enhancing spin–orbit coupling in the chromophore. On the other hand, fluorine substitution introduces large C–F bond dipoles into the chromophore, with the attendant possibility that specific solute–solvent interactions which perturb the radiationless decay rate could be present when using polar solvents. It would therefore seem prudent to use neither polar nor heavy atom-containing solvents when the rate data for fluorine-substituted molecules are analyzed.

Several possible energy gap law correlations were attempted using the data in Table 2, starting with the three rigid molecules, AZ, FAZ, and DFAZ. It is immediately apparent that no correlation exists between the S_2 – S_0 energy gap, $\Delta E(S_2$ – $S_0)$, and $\log(k_{nr})$, since the values of k_{nr} vary greatly while $\Delta E(S_2$ – $S_0)$ is almost constant for these three compounds. This observation rules out S_2 – S_0 internal conversion as a major S_2 decay process, at least for these thermalized molecules in solution. By contrast, an excellent linear relationship between $\log(\Sigma k_{nr})$ and $\Delta E(S_2$ – $S_1)$ is found for AZ in all six solvents, and for FAZ and DFAZ in the three most weakly interacting solvents (H, PFH/PFCH, and B). These results are displayed in Figure 3A; the equation of this straight line is

$$\log(k_{ic}) = 13.83 - (3.54 \times 10^{-4})\Delta E(S_2 - S_1) \quad (5)$$

where k_{ic} and ΔE are in units of s^{-1} and cm^{-1} , respectively; the correlation coefficient is $r^2 = 0.957$. The nonradiative decay constants for FAZ and DFAZ in the three more strongly interacting solvents, DCM, EtOH, and MeCN, follow the same general trend. However, because specific dipolar solute–solvent interactions can occur in these solvents the data for FAZ and DFAZ in DCM, MeCN, and EtOH were not used in the energy

gap correlation shown in Figure 3A even though doing so would have resulted in only marginal changes to the slope and correlation coefficient. Using only the C_{2v} molecules, AZ and DFAZ, also marginally improves the correlation, but there is no fundamental reason to eliminate the data for the C_s molecule, FAZ. It is interesting to note that a similar energy gap law plot for data taken on AZ alone in six similar solvents¹¹ exhibits exactly the same slope and intercept, within experimental error, as the line of Figure 3A; a similar plot for AZ- d_8 (not shown¹¹) has the same slope but an intercept which is slightly smaller owing to the deuterium isotope effect, $k_H/k_D = 1.3$. All of these data point to the fact that the nonradiative decay of the S_2 states of these rigid molecules occurs predominately by S_2 – S_1 internal conversion, and that log-linear energy gap law correlation is valid for this process in this system.

A similar plot of the nonradiative decay data for IAZ, IFAZ, and IDFAZ in *n*-hexane (Figure 3B) is also linear and exhibits a slope which is identical to that of the line in Figure 3A, within experimental error. The nonradiative decay rates of the S_2 states of these 6-isopropyl-substituted azulenes are consistently faster than their rigid counterparts for the same S_2 – S_1 electronic energy gaps, a phenomenon which has previously been termed the “loose bolt effect”.³⁰ Qualitatively, the additional group in the molecule increases the radiationless transition rate because its vibrations and hindered rotations couple with the vibrations of the rigid molecule, thereby providing a larger number of vibrational (or hindered internal rotational) states through which the two electronic states can interact. However, no quantitative estimation of this effect has been possible from previous data.

A comparison of the data displayed in Figure 3A for the AZ, FAZ, and DFAZ series with that of Figure 3B for the IAZ, IFAZ, and IDFAZ series show that a “loose bolt” like the isopropyl group substituted at the 6-position introduces the same quantitative proportional increase in S_2 's nonradiative decay rate in each of AZ, FAZ, and DFAZ. This increase must be due specifically to the isopropyl group since no other structural change has been introduced. This observation therefore suggests that Σk_{nr} for the S_2 states of IAZ, IFAZ, and IDFAZ can be expressed as the product of two factors,

$$\Sigma k_{nr} = k_{ic}(\text{rigid})f_{6\text{-ipr}} \quad (6)$$

where $k_{ic}(\text{rigid})$ is the rate constant for internal conversion of a rigid azulene molecule having a given $\Delta E(S_2$ – $S_1)$ and $f_{6\text{-ipr}}$ is the multiplicative factor which accounts for the additional coupling provided by the 6-isopropyl group for the same energy gap. Using this relationship, one obtains $f_{6\text{-ipr}} = 2.9$ from the data obtained here. A simple interpretation of this datum is that 2.9 is the factor by which the effective number of coupled states increases by substitution of the hindered rotating isopropyl group at the 6-position. That is, based on eq 3, $f_{6\text{-ipr}} = \rho_{6\text{-ipr}}/\rho_{6\text{-H}}$.

If this hypothesis is correct, a similar approach should be possible for other azulene derivatives in which H is replaced by substituents containing only light atoms, such as CH_3 – and other alkyl groups. Previous work in which estimates of k_{nr} have been obtained for some simple alkyl-substituted azulenes all provide qualitative support for this notion.^{5,6,8,9,11} Unfortunately, accurate S_2 lifetime and quantum yield data are not available for many of the compounds one might wish to use to test this hypothesis quantitatively; only 4,6,8-trimethylazulene (TMA) and guaiazulene (1,4-dimethyl-7-isopropylazulene, GAZ) have been measured.¹¹ For TMA, an S_2 lifetime of approximately 16 ps gives $k_{nr} \approx 6 \times 10^{10} s^{-1}$ in cyclohexane and perfluorocyclohexane¹¹ where $\Delta E(S_2$ – $S_1) \approx 12\,400 cm^{-1}$, yielding a value of $f_{CH_3} = 2.8$ per methyl group, assuming each one

contributes independently to the additional coupling. The only available value of k_{nr} for a monomethyl-substituted azulene is a crude estimate calculated from the oscillator strength of the S_2-S_0 transition for 2-methylazulene.⁵ Using this datum, a value of $f_{2-CH_3} = 1.4$ is obtained for 2-methyl substitution and $\Delta E(S_2 - S_1) \cong 13\,900\text{ cm}^{-1}$. Using these data for GAZ one would predict f_{GAZ} to be equal either to 23 ($2.8 \times 2.8 \times 2.9$) or 5.7 ($1.4 \times 1.4 \times 2.9$) for two independently acting methyl groups and one isopropyl group assuming the position at which the groups are substituted is not a factor; a value of $f_{GAZ} = 3.8$ is actually observed for $\Delta E(S_2 - S_1) = 13\,700\text{ cm}^{-1}$. Thus it is clear that, for a fixed energy gap, the effects on k_{nr} of multiple alkyl substitution are not obtained by simply multiplying the values of f for each substituent, irrespective of its position or other structural factors. The observed lack of additivity is consistent with the fact that the substituents are hindered rotors which cause slightly different distortions of the potential surfaces of each different molecule.

In addition, the rate constant for the nonradiative decay of 1,4-dimethyl-3-fluoro-7-isopropylazulene (FGAZ) is smaller than would be expected solely on the basis of the apparent reduction in $\Delta E(S_2 - S_1)$ caused by substitution of GAZ by one fluorine atom. Unfortunately, the large uncertainties in $\Delta E(S_2 - S_1)$ for GAZ and FGAZ make it impossible to do a quantitative analysis of this effect. Qualitatively, however, this too points to the need to account for not only the nature of the substituent but also its position when determining the quantitative effects of substitution.

In azulene derivatives containing heavy atoms, previous work^{5,6,11} has suggested that intersystem crossing to the triplet manifold becomes competitive with S_2-S_1 internal conversion, and is manifest in shorter S_2 lifetimes at a given $\Delta E(S_2 - S_1)$ than would be observed for azulenes containing only light atoms. These observations and their qualitative interpretation are verified by the present work. The operation of two parallel S_2 radiationless decay processes are accounted for by setting

$$\sum k_{nr} = k_{ic} + k_{isc} \quad (7)$$

For light-atom containing derivatives, $k_{ic} \gg k_{isc}$ and intersystem crossing contributes only marginally to S_2 's decay whereas k_{isc} and k_{ic} are of the same order of magnitude for compounds containing heavy atoms. Considering only first-order perturbations, symmetry-based selection rules³¹ suggest that $S_2(^1A_1)$ should couple more strongly with $T_1(^3B_1)$ than with $T_2(^3A_1)$, and an energy gap relation for the intersystem crossing process should therefore involve correlation of $\log(k_{isc})$ with $\Delta E(S_2 - T_1)$. Values of k_{isc} can be obtained by subtracting k_{ic} for the light-atom containing molecules at the same energy gap from $\sum k_{nr}$. However, values of the triplet state energies of these compounds are not known, and are difficult to establish with accuracy, so the $\Delta E(S_2 - T_1)$ are uncertain.

Fortunately, the S_1-T_1 energy gaps in all the azulene derivatives examined here are expected to be small, and approximately the same as that of azulene itself, namely $460 \pm 30\text{ cm}^{-1}$, a number which is known with some precision.³² The reasons for the small S_1-T_1 energy spacings are associated with the small LUMO-HOMO overlap, and the resulting small correlation energies for the two orbitally unpaired electrons in these states.²⁴ Thus, reasonable values of $\Delta E(S_2 - T_1)$ can be obtained by adding 460 cm^{-1} to the value of $\Delta E(S_2 - S_1)$ for each compound even though the triplet energies are difficult to obtain directly. If only structurally rigid molecules are compared, one can use the data for 1,3-dichloroazulene and 1,3-dibromoazulene and compare them with the data for structurally rigid

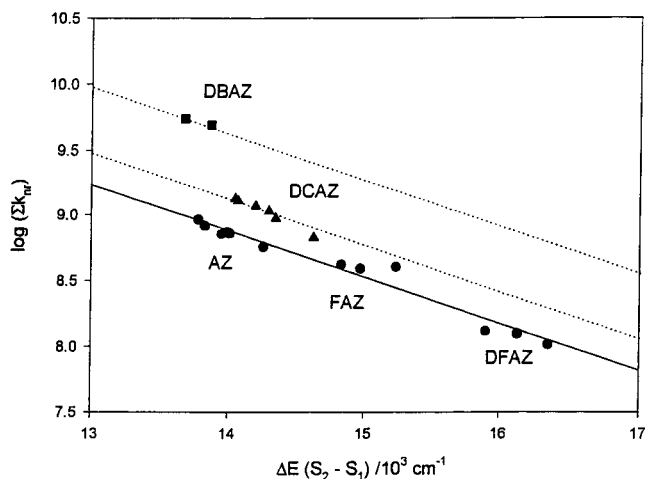


Figure 4. Log-linear energy gap law plots (see text) for AZ, FAZ, and DFAZ in several solvents and, for comparison, the same data for 1,3-dichloroazulene (DCAZ) and 1,3-dibromoazulene (DBAZ) taken from ref 11. The dotted lines are parallel to that of the linear regression for the rigid light-atom-containing molecules and are drawn to illustrate the interpretation of the data given in the text, i.e., $\sum k_{nr} = k_{ic} + k_{isc}$ at $\Delta E(S_2 - S_1) = 14\,000\text{ cm}^{-1}$.

TABLE 3: Contribution of the Different Decay Pathways for AZ, IAZ, DCAZ, and DBAZ at $\Delta E(S_2 - S_1) = 14\,000\text{ cm}^{-1}$

| compd | $\sum k_{nr}/10^8\text{ s}^{-1}$ | $k_{ic}(\text{rigid})/10^8\text{ s}^{-1}$ | f_{ipr} | $k_{isc}/10^8\text{ s}^{-1}^a$ |
|-------------------|----------------------------------|---|-----------|--------------------------------|
| AZ (FAZ, DFAZ) | 7.59 | 7.59 | | <1 |
| IAZ (IFAZ, IDFAZ) | 22.7 | 7.59 | 3.0 | |
| DCAZ | 12.9 | 7.59 | | 5.31 (41.2%) |
| DBAZ | 43.7 | 7.59 | | 36.1 (82.6%) |

^a The percentages are $(k_{isc}/\sum k_{nr}) \times 100$.

azulenes containing only light atoms in order to determine the effects of heavy atom substitution.

Plots of $\log(\sum k_{nr})$ vs $\Delta E(S_2 - S_1)$ using the data of Wagner et al. for DCAZ and DBAZ in several solvents¹¹ are shown in Figure 4, with the data for AZ, FAZ, and DFAZ determined here shown for comparison. Note that, for the same $\Delta E(S_2 - S_1)$, the nonradiative decay rates of DCAZ are slightly but consistently faster than those of similar structurally rigid molecules containing only C, H, and F, whereas the rates for the DBAZ derivative are substantially faster. The increase in rate is attributed to intersystem crossing and is determined quantitatively by applying eq 7 at fixed energy gap. A meaningful $\log(k_{isc})$ vs $\Delta E(S_2 - T_1)$ energy gap law correlation cannot be made with these data, however, because the solvatochromic shift in $\Delta E(S_2 - S_1)$ is small for each compound, and there is added uncertainty in determining $\Delta E(S_2 - T_1)$. Thus, we analyze instead the values of k_{isc} calculated for a fixed arbitrarily chosen energy gap, $\Delta E(S_2 - S_1) = 14\,000\text{ cm}^{-1}$ or $\Delta E(S_2 - T_1) \approx 14\,460\text{ cm}^{-1}$ where $k_{ic} = 7.6 \times 10^8\text{ s}^{-1}$; these data are given in Table 3.

The rate constant for intersystem crossing is approximately proportional to the square of the electronic matrix element for the spin-orbit coupling of the singlet and triplet states, which in turn is approximately proportional to the sum of the squares of the spin-orbit coupling constants, ζ , for the molecule's constituent atoms,²⁰ i.e.,

$$k_{isc} \propto C_{isc}^2 \propto \sum \zeta^2 \quad (8)$$

The proportionality between k_{isc} and $\sum \zeta^2$ can be tested for

TABLE 4: Analysis of Energy Gap Law plots ($\log(\sum k_{nr})$ vs ΔE) for Several Azulene Derivatives in Various Solvents

| system | slope/ 10^{-3} cm | intercept | γ | C/cm^{-1} |
|--------------------------------------|------------------------|-----------|----------|--------------------|
| AZ, FAZ, DFAZ in various solvents | -0.354 | 13.829 | 0.286 | 8.9 |
| AZ- d_8 in various solvents | -0.354 | 13.705 | 0.286 | 7.7 |
| IAZ, IFAZ, IDFAZ in hexane | -0.354 | 14.415 | 0.286 | 16.9 |
| DCAZ in various solvents | -0.354 | 14.065 | 0.286 | 12.1 |
| DBAZ in various solvents | -0.354 | 14.586 | 0.286 | 25.4 |

molecules of similar structure using the data in Table 4 and accepted values²⁰ of ζ . One finds for DCAZ and DBAZ at a fixed value of $\Delta E(S_2-T_1) = 14\,460\text{ cm}^{-1}$ that the ratio of the values of $k_{isc}(\text{DBAZ})/k_{isc}(\text{DCAZ}) = 6.8$, whereas the comparable ratio of $\sum \zeta^2 = 17$. Agreement is semiquantitative, but at least as good as other similar correlations of the heavy atom effect.

Finally, we can calculate the electronic matrix elements for S_2-S_1 coupling from the data in Table 2. For two weakly coupled states, Englman and Jortner¹³ have derived the following relationship between k_{ic} and the electronic energy gap, ΔE , between them:

$$k_{nr} = \frac{(2\pi)^{1/2} C^2}{\hbar(\hbar\omega_M \Delta E)^{1/2}} \exp\left\{-\left(\frac{\gamma}{\hbar\omega_M}\right)\Delta E\right\} \quad (9)$$

where

$$\gamma = \ln\left\{\frac{2\Delta E}{\sum_M \hbar\omega_M \Delta_M^2}\right\} - 1 \quad (10)$$

Here C_{ic} is the matrix element for vibronic coupling between the two states, and $\hbar\omega_M$ and Δ_M are the energy and reduced displacement of the accepting vibrational modes, M . Differentiation of the logarithm of (9) with respect to ΔE yields

$$\frac{d(\ln k_{nr})}{d(\Delta E)} = -\frac{1}{2\Delta E} - \left(\frac{\gamma+1}{\hbar\omega_M}\right) \quad (11)$$

$$\frac{d(\log k_{nr})}{d(\Delta E)} = -\frac{\gamma+1}{2.3\hbar\omega_M} \quad (12)$$

which allows γ to be determined from the measured slopes of $\log(k_{ic})$ vs ΔE plots such as Figure 3. The $-1/(2\Delta E)$ term in eq 11 is often neglected¹¹ since the range of ΔE is small, and eq 12 was therefore used in the present calculations. The slope of the linear regression of Figure 3 for the AZ, FAZ, and DFAZ series was used for the γ calculations. Since the slope is the same for every series, the γ value is also identical. Once γ is obtained, C can be calculated directly from any given ΔE and k_{nr} values for any assumed value of $\hbar\omega_M$.

Griesser and Wild^{8,9} found that perdeuterating azulene had a very small effect on $\sum k_{nr}$ ($k_H/k_D = 1.57$ in ethanol) and argued convincingly that this demonstrated that in-plane skeletal C-C, not high-frequency C-H(D), stretching vibrations are the important accepting modes in S_1 . Wagner et al.¹¹ confirmed this interpretation and did a more accurate measurement ($k_H/k_D = 1.30$ in ethanol). Accordingly, if Griesser and Wild's value of $\hbar\omega_M = 1580\text{ cm}^{-1}$ for the wavenumber of an "average" aromatic C-C stretching vibration is employed, and all the energy gap law plots are assumed to have the same slope, the calculation of γ and C_{ic} using eqs 12 and 9 gives the results shown in Table 4.

For the AZ, FAZ, and DFAZ series, $\gamma = 0.286$ and $C_{ic} = 8.9\text{ cm}^{-1}$. This value of C_{ic} is rather small, compared with the range of values found for internal conversion in other systems,³³ and points to rather weak coupling between S_2 and S_1 in this system. For molecules belonging to the C_{2v} point group, S_2 and S_0 are of A_1 symmetry whereas S_1 is B_1 (using the non-Mulliken convention). The S_1 surface is displaced from S_0 by a very substantial compression of the central C(9)-C(10) bond and an elongation of the other C-C bonds involving these two atoms, a deformation which results in the conical intersection of the S_1 and S_0 surfaces.³⁴ However, the magnitude of the electronic matrix element, C_{ic} , suggests that S_1 and S_2 are weakly coupled and that the surfaces therefore remain "nested" at the energies probed in the present experiments.

Conclusions

The UV-visible-near-IR absorption spectra, $S_2 \rightarrow S_0$ fluorescence quantum yields and S_2 fluorescence lifetimes of 1-fluoroazulene, 1,3-difluoroazulene, and several of their alkyl-substituted derivatives have been measured in up to six solvents, benzene, dichloromethane, ethanol, acetonitrile, *n*-hexane, and perfluoro-*n*-hexane. The $S_2 \rightarrow S_0$ fluorescence quantum yields and S_2 lifetimes of 1,3-difluoroazulene are exceptionally large—the largest ever reported for an upper excited singlet state of a polyatomic organic molecule in solution at room temperature.

The nonradiative rate constants for the decay of the S_2 states of these molecules in these solvents and of azulene, 1,3-dichloroazulene and 1,3-dibromoazulene, determined previously by Wagner et al.,¹¹ have been analyzed in terms of the weak coupling case of radiationless transition theory. The data show that the nonradiative rate constants for the S_2 states of azulene, 1-fluoroazulene, and 1,3-difluoroazulene in the nonpolar solvents follow the log-linear relationship expected of the energy gap law, provided that S_2-S_1 internal conversion is assumed to dominate the decay mechanism. The same linear correlation is obtained, irrespective of whether $\Delta E(S_2-S_1)$ is varied by solvatochromism or fluorine substitution.

Substitution by alkyl groups increases the nonradiative decay rates by increasing the effective number of coupled states while the electronic coupling matrix element remains constant. Substitution at the 6-position by an isopropyl group increases the rate constant by a constant factor of 2.9; however, multiple substitution does not have a multiplicative effect. Substitution by chlorine or bromine increases the S_2 decay rates by enhancing the rate of intersystem crossing to the triplet manifold. The rate enhancement is semiquantitatively modeled by considering the effects of spin-orbit coupling of the halogen atoms.

Acknowledgment. This work was supported in part by the grants from the US Army Research Office (DAAH04-96-1-0031 to R.S.H.L.) and the Natural Sciences and Engineering Research Council of Canada (to R.P.S.). N.T. is grateful for a summer scholarship under the RISE program.

References and Notes

- Beer, M.; Longuet-Higgins, H. C. *J. Chem. Phys.* **1955**, *23*, 1390.
- Kasha, M. *Discuss. Faraday Soc.* **1950**, *9*, 14.
- Binsch, G.; Heilbronner, E.; Jankow, R.; Schmidt, D. *Chem. Phys. Lett.* **1967**, *1*, 135.
- Murata, S.; Iwanga, C.; Toda, T.; Kokubun, H. *Chem. Phys. Lett.* **1972**, *13*, 101; erratum **1972**, *15*, 152.
- Murata, S.; Iwanga, C.; Toda, T.; Kokubun, H. *Ber. Bunsenges. Phys. Chem.* **1972**, *76*, 1176.
- Eber, G.; Schneider, S.; Dörr, F. *Chem. Phys. Lett.* **1977**, *52*, 59.
- Gillispie, G. D.; Lim, E. C. *Chem. Phys. Lett.* **1979**, *63*, 193.
- Griesser, H. J.; Wild, U. P. *Chem. Phys.* **1980**, *52*, 117.
- Griesser, H. J.; Wild, U. P. *J. Photochem.* **1980**, *12*, 115.

- (10) Sobolewski, A. L.; Prochorow, J. *J. Lumin.* **1984**, 31/32, 589.
- (11) Wagner, B. D.; Tittelbach-Helmrich, D.; Steer, R. P. *J. Phys. Chem.* **1992**, 96, 7904.
- (12) Klemp, D.; Nickel, B. *Chem. Phys. Lett.* **1986**, 130, 493.
- (13) Englman, R.; Jortner, J. *Mol. Phys.* **1970**, 18, 145.
- (14) Hirata, Y.; Lim, E. C. *J. Chem. Phys.* **1978**, 69, 3292.
- (15) Meech, S. R.; Phillips, D. *J. Photochem.* **1983**, 23, 193.
- (16) Muthyala, R. S.; Liu, R. S. H. *J. Fluorine Chem.* **1998**, 89, 173.
- (17) Maciejewski, A.; Steer, R. P. *J. Photochem.* **1986**, 35, 59.
- (18) James, D. R.; Demmer, D. R. M.; Verrall, R. E.; Steer, R. P. *Rev. Sci. Instrum.* **1983**, 54, 1121.
- (19) Szymanski, M.; Steer, R. P. *J. Phys. Chem.* **1992**, 96, 8720.
- (20) McGlynn, S. P.; Azumi, T.; Kinoshita, M. *Molecular Spectroscopy of the Triplet State*; Prentice Hall: Englewood Cliffs, NJ, 1969.
- (21) Lacey, A. R.; McCoy, E. F.; Ross, I. G. *Chem. Phys. Lett.* **1973**, 21, 233.
- (22) Lawrance, W. D.; Knight, A. E. W. *J. Phys. Chem.* **1990**, 94, 1249.
- (23) (a) Michl, J.; Thulstrup, E. W. *Tetrahedron* **1976**, 32, 205. (b) Klessinger, M.; Michl, J. *Excited States and Photochemistry of Organic Molecules*; VCH Publishers: New York, 1995; p 104.
- (24) Abou-Zied, O. K.; Sinha, H. K.; Steer, R. P. *J. Phys. Chem. A* **1997**, 101, 7989.
- (25) Strickler, S. J.; Berg, R. A. *J. Chem. Phys.* **1962**, 37, 814.
- (26) Orlandi, G.; Siebrand, W. *J. Chem. Phys.* **1973**, 58, 4513.
- (27) Freed, K. F. *Top. Curr. Chem.* **1972**, 31, 105.
- (28) Turro, N. J.; Ramamurthy, V.; Cherry, W.; Farneth, W. *Chem. Rev.* **1978**, 78, 126.
- (29) Siebrand, W.; Williams, D. F. *J. Chem. Phys.* **1968**, 49, 1860.
- (30) Turro, N. J. *Modern Molecular Photochemistry*; Benjamin: New York, 1978; p 170.
- (31) Hochstrasser, R. M. *Molecular Aspects of Symmetry*; Benjamin: New York, 1966, Chapter 9.
- (32) Nickel, B.; Klemp, D. *Chem. Phys.* **1993**, 174, 319.
- (33) Hochstrasser, R.; Marzacco, C. *J. Phys. Chem.* **1968**, 49, 971.
- (34) Bearpark, M. J.; Bernardi, F.; Clifford, S.; Olivucci, M.; Robb, M. A.; Smith, B. R.; Vreven, T. *J. Am. Chem. Soc.* **1996**, 118, 169.